Heliyon 9 (2023) e12492

Contents lists available at ScienceDirect

Heliyon

journal homepage: www.cell.com/heliyon

Research article

Rational synthesis, biological screening of azo derivatives of chloro-phenylcarbonyl diazenyl hydroxy dipyrimidines/ thioxotetrahydropyrimidines and their metal complexes

Tariq Aziz [a,1], Hafiza Ammara Nasim [a,1], Khalil Ahmad [b,c,*], Habib-ur-Rehman Shah [a], Sajidah Parveen [a], Muhammad Mahboob Ahmad [d], Hammad Majeed [b], Ahmad M. Galal [e,f], Abdul Rauf [a], Muhammad Ashfaq [a,**]

[a] Institute of Chemistry, Baghdad ul Jadeed Campus, The Islamia University of Bahawalpur, Bahawalpur, 63100, Pakistan
[b] University of Management and Technology (UMT) Sialkot Campus, Sialkot, Punjab, Pakistan
[c] Cholistan University of Veterinary and Animal Sciences (CUVAS), Bahawalpur, Punjab, Pakistan
[d] Institute of Chemical Sciences, Bahauddin Zakariya University Multan, Pakistan
[e] Department of Mechanical Engineering, College of Engineering in Wadi Alddawasir, Prince Sattam Bin Abdul-Aziz University, Al-Kharj, 16278, Saudi Arabia
[f] Production Engineering and Mechanical Design Department, Faculty of Engineering, Mansoura University, Mansoura P.O. 35516, Egypt

ARTICLE INFO

Keywords:
Azo compounds
Antimicrobial agents
Antioxidant
Metal complexes

ABSTRACT

Herein, a new series of azo ligands HL-1 *(5-(2-chloro-6-(phenylcarbonyl)phenyl)diazenyl)-6-hydroxydihydropyrimidines-2,4dione)*, HL-2 *(5-(2-chloro-6-(phenylcarbonyl)phenyl)diazenyl)-6-hydroxy-2-thioxottetrahydropyrimidin-4one)*, HL-3 *(5-(2,4-dichloro-6-(phenylcarbonyl)phenyl) diazenyl)-6-hydroxydihydropyrimidines-2,4dione)*, HL-4 *(5-(2,4-dichloro-6-(phenylcarbonyl) phenyl) diazenyl)-6-hydroxy-2-thioxotetrahydropyrimidin-4one)* and their metal complexes with Cu(II) & Ni (II) were synthesized successfully having excellent yield, in reproducible conditions and for structure elucidation different advance spectroscopic techniques (FTIR, ^{1}H NMR, ^{13}C NMR and Mass Spectrometry) were applied. In FTIR analysis, the absence of peak at *3450-3550 cm^{-1}* due to $-NH_2$ and presence of a new peak of N=N at 1390-1520 cm^{-1} confirmed synthesis of the ligands. The ^{1}H NMR spectra of azo ligands showed singlet peak at 11.5–13.5 ppm (Ar-OH) for hydroxyl group and $-NH_2$ signals disappearance of anilines at 4–5 ppm also gives strong indication for the synthesis of azo compounds. On complexation two most important peaks (M-O, M-N) appeared in all the metal chelates in the range of 400–600 cm^{-1} which were not present in any of the ligands, confirmed the formation of complexes. Molecular ion peaks in mass spectra at 273, 388, 407 and 423 m/z value for ligands as well as for complexes at 803, 835, 871 and 904 m/z also give strong indication that proposed ligands and their metal complexes are produced successfully. Biological screening of the synthesized compounds were also carried out against different bacterial strains (*E.coli*, *S.typhi*, and *B.subtilis)*, antifungal (*C.albicans*, *A.niger*, and *C.glabrata)* strains and antioxidant activity. From results it was observed that HL-4 and Cu complexes exhibited maximum inhibition against all bacterial and fungal strains as compared to other ligands and standard drug.

* Corresponding author.
** Corresponding author.
E-mail addresses: khalilnoorpur@gmail.com (K. Ahmad), chashfaqiub@yahoo.com (M. Ashfaq).
[1] These authors have equal contribution.

https://doi.org/10.1016/j.heliyon.2022.e12492
Received 5 November 2022; Received in revised form 13 November 2022; Accepted 13 December 2022
Available online 27 December 2022

1. Introduction

The emergence of multi-drug resistant (MDR) pathogens is the current issue now a days that the modern biochemists have been facing for many decades [1, 2]. Because of exceptional applications of drugs based on pyrimidine have been extensively studied in current years. Derivatives of pyrimidine are very proficient for antibacterial, antitumor, anti-HIV agent [3, 4, 5]. They also used in hypnotic drugs and diagnosis of cancer. Over the previous five decades, azo compounds having heterocyclic moiety played an imperative function in the expansion of azo coordination compounds because of their glorious claims in many fields like medicinal, biological, analytical and industrial research as they have extensive conjugation and easily existing lone pair of electrons [6]. Heterocyclic azo compounds and their metal chelates have been broadly studied because of their antimicrobial as well as antioxidant activities. Heterocyclic azo derivatives are well known for their pharmaceutical worth, familiar for their use as antidiabetics, antibacterial, antituberculosis, antitumor, antineoplastic, antiseptics and are famous to be participated in various biological reactions [7, 8, 9] *e.g* synthesis of protein, nitrogen fixation inhibition of RNA, DNA and HIV inhibitors of viral replications because azo derivatives bind with the reverse transcriptase and protease of retrovirus [10, 11, 12, 13, 14]. 3-aryl-azo-4-hydroxy coumarin and their Ni(II) and Co(II) metal complexes showed excellent antibacterial and antifungal activities [15, 16, 17, 18]. The Ni(II) and Cu(II) metal complexes with azo derivatives based upon phenazone displayed outstanding activity against Gram negative and Gram-positive bacteria than free ligands. Heterocyclic azo derivatives of sulfamethoxazole exhibited brilliant antituberculosis activity against *Mycobacterium tuberculosis* [19, 20, 21, 22]. Azo derivatives of salicylic acid displayed cytotoxic, antioxidant, antiviral, antimalarial and antiproliferative activities since 40 years [23, 24, 25, 26].

Azo derivatives have variety of applications as remedial agents in polypeptides activities, in enzymes modifications and in diagnosis of Alzheimer's disease. Naphthalene based azo derivatives expressed many biological applications such as HIV-1 integrase inhibitory activities [27, 28, 29]. Heterocyclic series of mono-azo dyes are exhibiting considerable antimicrobial activities against fungi and bacteria [30]. Many azo compounds are important for biomedical and medicinal research as an anticoagulant, antiproliferative, antioxidant, antibacterial, antihypertensive and antifungal agents [31, 32, 33, 34]. Polymers based on azo dyes are under study in many countries for the treatment of liver, colon diseases as well as their cancer. Azo derivatives of rhodamine and their metal complexes with transition metals are tangled in biochemical processes and reactions including antimicrobial activities against fungi, bacteria and DNA inhibition activities [9, 35, 36, 37]. There are many derivatives of heterocyclic azo compounds like as pyrimidine azo derivatives which can easily coordinated with metals and form ring structure metal complexes, applied as cationic and anionic bio sensors [38, 39, 40].

In this study, a new series of heterocyclic azo compounds were produced using 4, 6-dihydroxy-2-thiopyrimidine and 4, 6-dihydroxypyrimidine as coupling reagent. In a consequence, the current work is performed for the study of structural elucidation of the synthesized pyrimidine azo compounds/derivatives by different techniques such as FTIR, ^{1}H NMR, ^{13}C NMR, and mass spectrometry. Further these synthesized compounds were screened against bacteria, fungus and antioxidant potential.

2. Experimental

2.1. Materials

Barbituric acid, thio-barbituric acid, 2-methyl aniline, 2-nitro aniline, hydrochloric acid and sodium hydroxide of Merck and BDH were purchased and used as such without further purification. Solvents such as DMSO, DCM, CCl_4, n-hexane, ethanol, methanol and water were used after double distillation.

2.2. Instrumentation

FTIR spectrophotometer BRUKER Tensor 27 were used by ATR technique in the range of 600–4000 cm^{-1} at room temperature. For ^{1}H NMR and ^{13}C NMR spectra BRUKER 300 MHz were used having $CDCl_3$ as internal reference solvent. JEOL JMS 600-H instrument were used for recording MS spectra.

2.3. Synthetic procedure for azo ligands: (Diazotization and coupling)

Azo ligands of barbituric acid and thio-barbituric acid have been synthesized by diazotization and coupling reaction by adopting the previous procedure [41] with minor modifications as given in (Scheme 1). In a typical method 30 mmol of aniline (3-chloro-2-aminobenzophenone and 3,5-dichloro-2-aminobenzophenon) was dissolved in a mixture of 30 mL distilled water and 5 mL of 12 M HCl with continuous cooling and stirring until temperature decreased to 0–5 °C. Then freshly prepared 30 mmol aqueous solution of sodium nitrite added drop wise in above solution with constant stirring until yellow color benzophenone diazonium chloride was formed in ice bath. Resulting diazonium chloride solution was added drop wise in a reaction flask having 30 mmol of freshly prepared solution of coupling reagent (barbituric acid and thio-barbituric acid] at 0–5 °C. The color of mixture was changed from yellow to reddish brown and reaction was completed in 3 hr with constant stirring below 0–5 °C. Reddish brown precipitates of azo ligands (HL1-HL4) were filtered out and washed several times with hot water and ethanol mixture. Monitoring of reaction and purification of products was confirmed using TLC.

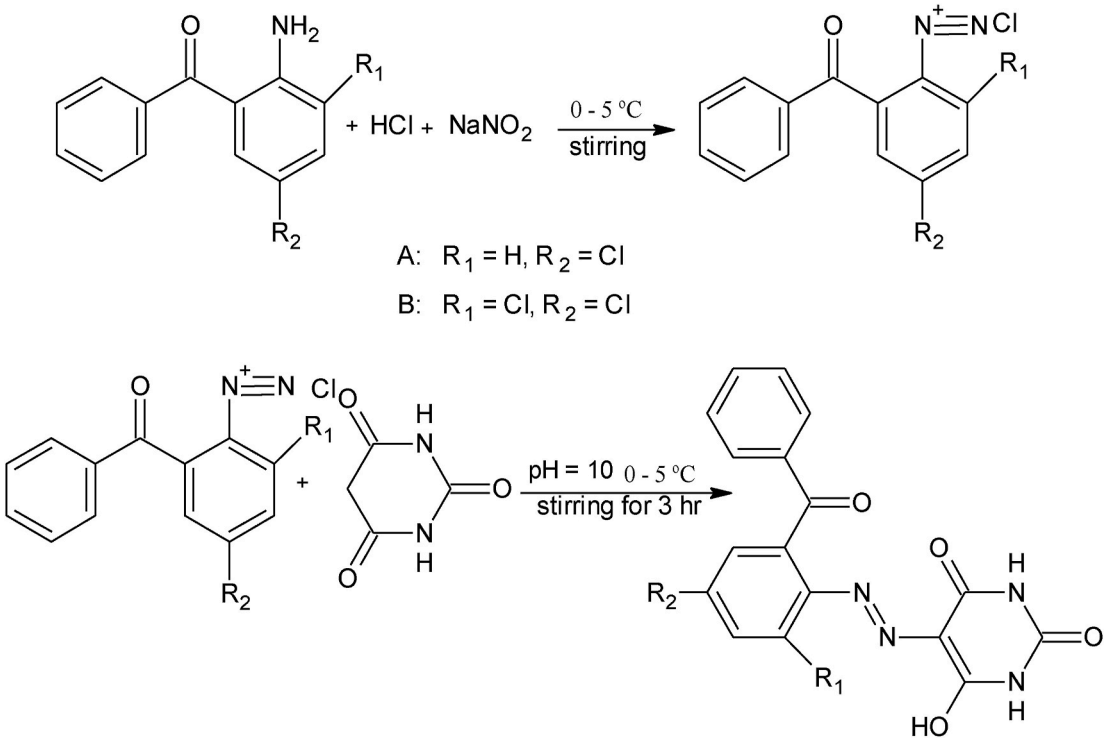

Scheme 1. Synthetic Route of Azo Ligands.

2.3.1. *Physical properties and characterization data of ligands*

2.3.1.1. HL-1 (5-(2-chloro-6-(phenyl carbonyl) phenyl) diazenyl)-6 hydroxydihydropyrimidines-2,4dione). M.P: 189 °C, Color: Red, Yield: 60%, Solubility: C_2H_5OH, CH_3OH, DMSO. FTIR (cm^{-1}): N=N: 1508.56s; NH: 3445.54s: OH: 3161.13b; CH sp_2: 3021.64w; C=O: 1602.65s; C–O: 1256.03; Cl: 818.56s and 750sp (Figure 1a). ^1H NMR (DMSO) δ ppm OH (1H): 11.235; aryl protons (8H): 6.22–7.35m NH (2H): 9.23–9.21 (Figure 1b). ^{13}C NMR (DMSO) δ ppm: C–OH (1C): 190.14; C=O: (3C):160.90–163.49; C–N: 1O4; C–Cl: 1O4.49, C-phenyl: 121-140 (Figure 1c). MS m/z: $(C_{17}H_{13}ClN_4O_7)^+$ M^+ 372.82; $(C_{17}H_{14}N_4O_7)^+$ M^+ 338.13; $(C_{10}H_{10}N_4O_3)^+$ M^+ 234.27; $(C_{13}H_{10}ClNO)^+$ M^+ 231.18; $(C_7H_6O)^+$ M^+ 106.12; $(C_4H_7N_3O_3)^+$ M^+ 145.18; $(C_3H_7NO_2)^+$ M^+ 89.67; $(C_6H_6)^+$ M^+ 78.11 (Figure 1d).

2.3.1.2. HL-2 (5-(2-chloro-6-(phenyl carbonyl) phenyl) diazenyl)-6-hydroxy-2-thioxottetrahydr opyrimidin-4one). M.P: 221 °C; Color: brown; Yield: 63%; Solubility: C_2H_5OH, CH_3OH, DMSO. FTIR (cm^{-1}): N=N: 1441.27s; NH: 3456.90w; OH: 3255.49b; CH Sp_2: 3024.49w; C=O: 1601.17s; C=S: 1255.49w: Cl: 832.21s (Fig S1). ^1H NMR (DMSO) ppm δ: OH (1H): 11.25; NH (2H): 9.20–9.25; Aryl proton (8H): 6.26–7.35 (Fig S4). ^{13}C NMR (DMSO) ppm δ: C–OH (1C):189.03; C=O (3C): 161.06–161.93; C–CN: 105; C-aryl: 123-150 (Fig S7). MS, m/z: $(C_{17}H_{12}ClN_4O_3S)^+$ M^+ 407.20; $(C_{17}H_{14}N_4O_3S)^+$ M^+ 338.13; $(C_{10}H_{10}N_4O_3S)^+$ M^+ 234.12; $(C_{14}H_9Cl_2NOS)^+$ M^+ 266.12; $(C_{13}H_{10}OS)^+$ M^+ 182.0; $(C_4H_7N_3O_3)^+$ M^+ 145.11 $(C_3H_7NO_2)^+$ M^+ 89.67; $(C_6H_6)^+$ M^+ 77.15 (Fig S10).

2.3.1.3. HL-3 (5-(2,4-dichloro-6-(phenyl carbonyl) phenyl) diazenyl)-6-hydroxydihydropyrimi- dines-2,4dione). M.P: 239 °C; Color: Orange; Yield: 56%; Solubility: C_2H_5OH, CH_3OH, DMSO; FTIR: (cm^{-1}) N=N: 1510.90 m; NH: 3453w; OH: 3274.50b; CH Sp_2: 3168.35w; C=O: 1598.90s; C–O: 1168.35w; Cl; 698.34s (Fig S2). ^1H NMR (DMSO) ppm δ: OH (1H): 12.35; NH (2H): 9.01–9.51; Aryl proton (8H): 6.237–8.01 (Fig S5). ^{13}C NMR (DMSO) ppm δ: C–OH: 199; C=O: 160-162; C-aryl: 121-150; C–Cl: 100 (Fig S8). MS, m/z: $(C_{17}H_{12}Cl_2N_4O_4)^+$ M^+ 407.20; $(C_{17}H_{14}N_4O_4)^+$ M^+ 338.15 $(C_{10}H_{10}N_4O_3)^+$ M^+ 234.12; $(C_{13}H_9C_{l2}NO)^+$ M^+ 266.12 $(C_4H_7N_3O_3)^+$ M^+ 145.11; $(C_7H_5Cl_2NO)^+$ M^+ 190.02; $(C_6H_6)^+$ M^+ 77.12 (Fig S11).

2.3.1.4. HL-4 (5-(2,4-dichloro-6-(phenyl carbonyl) phenyl) diazenyl)-6-hydroxy-2-thioxotetra- hydropyrimidin-4one). M.P: 283 °C; Color: yellow; Yield: 67%; Solubility: C_2H_5OH, CH_3OH, DMSO. FTIR (cm^{-1}) N=N: 1446.71s; NH: 3401.18w; OH: 3241.45b; CH Sp_2: 3193.71w; C=O: 1592.36s; C–O: 1241.34s; Cl: 778.66s; C=S: 1196.49 (Fig S3). ^1H NMR (DMSO) ppm δ: OH (1H): 11.235; NH (2H): 9.44–9.52; Aryl-H (8H): 6.230–7.325 (Fig S6). ^{13}C NMR (DMSO) ppm δ: C–OH: 190; C=O: 160-165; C-aryl: 125-150; C–N: 100; C–Cl: 119 (Fig S9). MS, m/z: $(C_{17}H_{12}CL_2N_4O_3S)^+$ M^+ 423.27; $(C_{17}H_{14}N_4O_3S)^+$ M^+ 354.38; $(C_{10}H_{10}N_4O_2S)^+$ M^+ 250.27; $(C_{13}H_9Cl_2NO)^+$ M^+ 266.12; $(C_4H_7N_3O_2S)^+$ M^+ 161.35; $(C_6H_6)^+$ M^+ 77.13; $(C_3H_7NO_2)^+$ M^+ 89.09 (Fig S12).

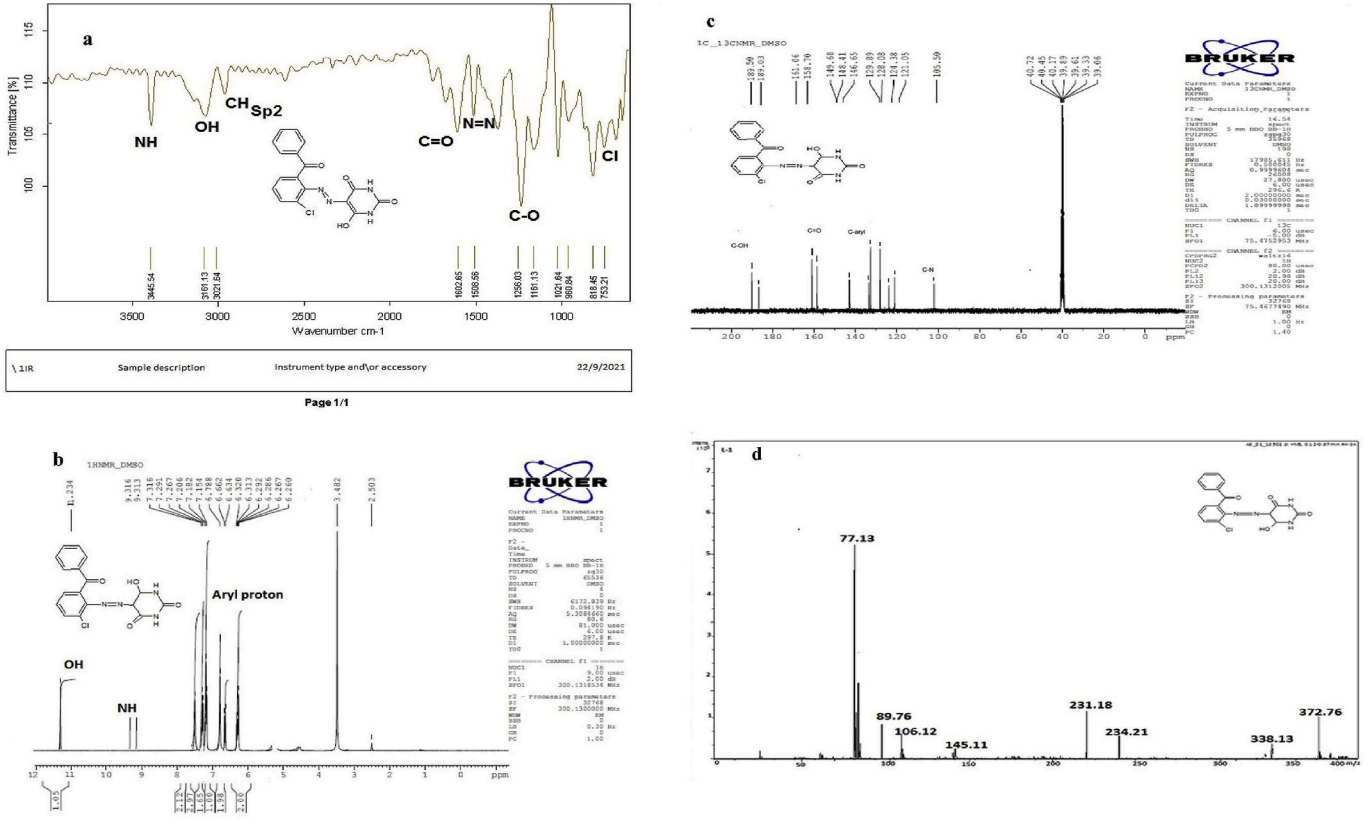

Figure 1. a) FTIR spectrum of ligand HL-1. b) 1HNMR spectrum of ligand HL-1. c) C13 NMR spectrum of ligand HL-1. d) Mass spectrum of ligand HL-1.

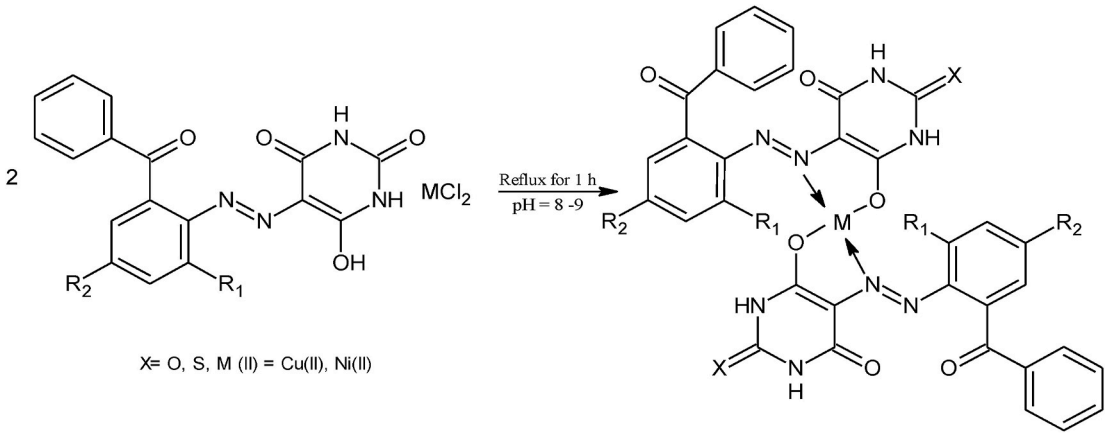

Scheme 2. Synthetic Route of Metal Complexes.

2.4. Synthetic procedure of azo metal complexes (Metallization)

The metal chelates were synthesized according to the procedure followed by H. Ammara et al [42] and K. Ahmad et al [41] with some modifications at pH = 8 as given in Scheme 2. Azo ligands (2 mmol) were dissolved in ethanol (30 mL) and then solution of metal chlorides also added (1mmol) Cu(II), Ni(II), Zn(II), Mn(II)) color changes at once. Then reaction mixture was refluxed for 1h until solid color complexes precipitated out and then left for 24 hr. Solid chelates were filtered out and washed several times with water and ethanol.

2.5. Physical properties and characterization data of metal complexes

2.5.1. L-1-Cu complex

M.P: 296 °C; Color: Orange; Yield: 51%; Solubility: C_2H_5OH, DMSO. FTIR (cm^{-1}): NH: 3452.66; CH sp_2; 3091.07; C=O: 1679 N=N: 1537; Cl: 750.81: Cu–N: 501; Cu–O: 455 (Figure 2). MS, m/z: $(C_{34}H_{20}Cl_2Cu– N_8O_8)^+$ M^+ 803.03; $(C_{34}H_{22}CuN_8O_8)^+$ M^+ 734.12; $(C_{20}H_{14}CuN_8O_6)^+$ M^+ 525.92; $(C_6H_8CuN_8O_6)^+$ M^+ 373.72; $(C_4H_5CuN_4O_2)^+$ M^+ 204.65; $(C_4H_6N_4O_2)^+$ M^+ 142.11; $(C_4H_7N_3O_2)^+$ M^+ 129.11; $(C_4H_7O)^+$ M^+ 113.21; $(Cu)^+$ M^+ 63 (Figure 3).

2.5.2. L-1-Ni complex

M.P: >300 °C: Color: Brown: Yield: 65%: Solubility: DMSO. FTIR (cm^{-1}): NH: 3306; CH Sp_2: 3093.20; C=O: 1662.56; N=N: 1464 Cl: 787; Ni–O: 592; Ni–N: 434 (Fig S13).

2.5.3. L-2-Cu complex

M.P: 299 °C; Color: light yellow; Yield: 45%; Solubility: DMSO. FTIR (cm^{-1}): NH: 3195.95s; $CHSp_2$: 3293.25; C=O: 1679.23; N=N: 1446.71C = S: 1241; C–N: 1196; Cl: 869; Cu–O: 592 Cu–N: 464 (Fig S14). MS, m/z: $(C_{34}H_{20}Cl_2CuN_8O_6S_2)^+$ M^+ 835.02; $(C_{34}H_{20}CuN_8O_6)^+$ M^+ 752.12; $(C_{20}H_{14}CuN_8O_4S_2)^+$ M^+ 558.92; $(C_8H_6CuN_8O_4S_2)^+$ M^+ 405.72; $(C_4H_5CuN_4OS)^+$ M^+ 220.65 $(C_4H_4N_4O_2)^+$ M^+ 142.11; $(C_4H_7N_3O_2)^+$ M^+ 129.11 $(C_4H_7N_3O)^+$ M^+ 113.21; $(Cu)^+$ M^+ 63 (Fig S20).

2.5.4. L-2-Ni complex

M.P: >300 °C; Color: Bright yellow; Solubility: DMSO. FTIR (cm^{-1}): NH: 3430; CH Sp_2: 3198 C=O: 1745; N=N; 1511; Cl: 834; Ni–O: 511; Ni–N: 430 (Fig S15).

2.5.5. L-3-Cu complex

M.P: 289 °C; Color: orange; Yield: 56%; Solubility: DMSO, FTIR (cm^{-1}): NH: 3306; $CHSp_2$: 3212.52; C=O: 1662; N=N: 1564; C–N: 1143; Cl: 868; Cu–O: 593.1; Cu–N: 512.45 (Fig S16). MS, m/z: $(C_{34}H_{18}Cl_4N_8O_6S_2)^+$ M^+ 871.0; $(C_{34}H_{22}CuN_8O_6S_2)^+$ M^+ 734.0; $(C_{20}H_{14}CuN_8O_6)^+$ M^+ 525.92; $(C_{14}H_{10}Cu– N_8O_6)^+$ M^+ 4 49.85; $(C_{13}H_{10}CuN_6O_5)^+$ M^+ 393.80, $(C_7H_6CuN_6O_5)^+$ M^+ 317.70 $(C_4H_4N_4O_3)^+$ M^+ 156.80; $(C_3H_3CuN_2O_2)^+$ M^+ 162.61; $(C_3H_3N_2O_2)^+$ M^+ 100; $(C_6H_6)^+$ M^+ 78.11; $(Cu)^+$ M^+ 63; $(C_3H_3)^+$ M^+ 42 (Fig S21).

2.5.6. L-3-Ni complex

M.P: >300 °C; Color, Brown; Yield: 45% Solubility: DMSO. FTIR (cm^{-1}): NH: 3347; CH Sp_2: 3043; C=O: 1728; N=N: 1594; Cl: 764; Ni–O: 591; Ni–N: 435 shown in Fig S17.

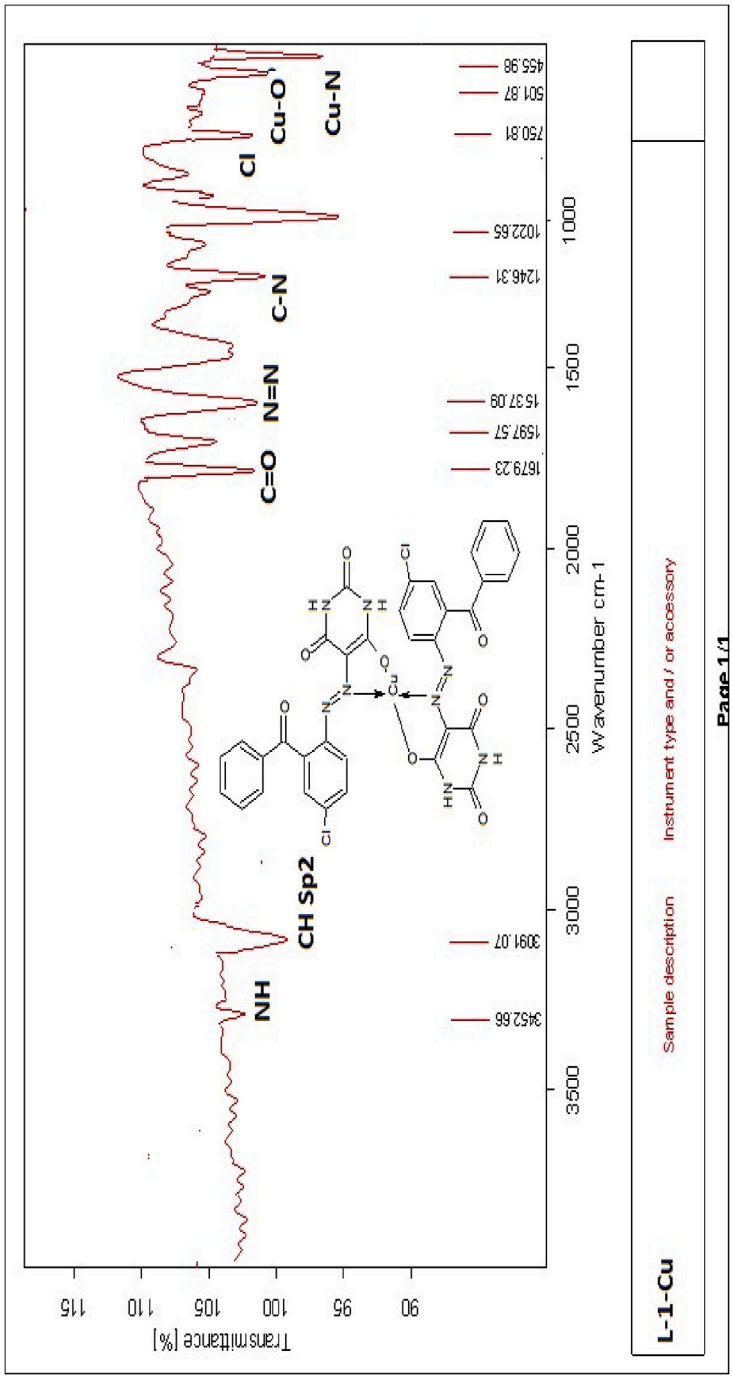

Figure 2. FTIR spectrum of HL1-Cu.

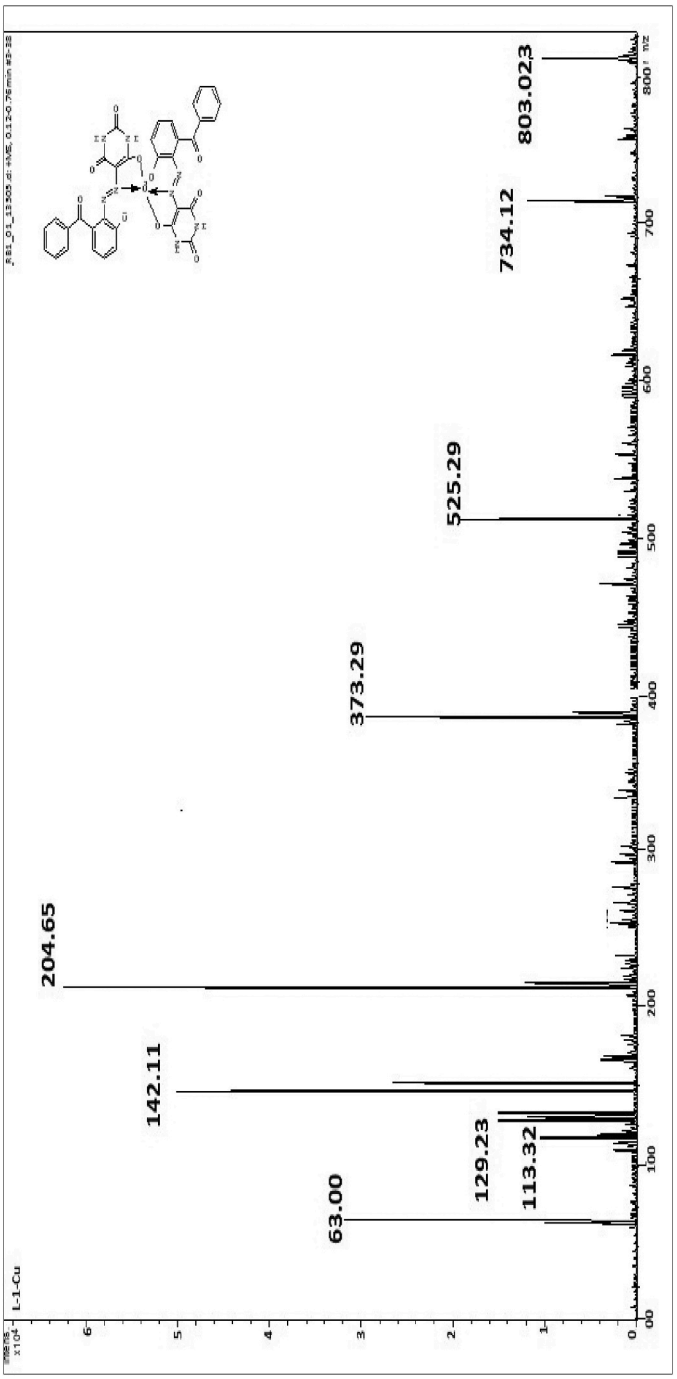

Figure 3. Mass spectrum of HL1-Cu.

2.5.7. L-4-Cu complex

M.P: 290 °C; Color: light green; Yield: 43%; Solubility: DMSO. FTIR (cm^{-1}): NH: 3377.64; CH Sp_2: 3087.14; C=O: 1727.87; N=N: 1511.54; Cu–O: 511.54; Cu–N: 424.58; Cl: 875 (Fig S18). MS, m/z: $(C_{34}H_{18}Cl_4CuN_8O_6S_2)^+$ M+ 904; $(C_{34}H_{22}CuN_8O_6S_2)^+$ M^+ 766.12; $(C_{20}H_{22}CuN_8O_4)^+$ M^+ 558; $(C_{14}H_{10}Cu–\ N_8O_4S_2)^+$ M^+ 481.85; $(C_{13}H_{10}CuN_6O_4S)^+$ M^+ 408.81; $(C_7H_6CuN_6O_4S)^+$ M^+ 333.70; $(C_4H_4N_4O_2S)^+$ M^+ 165.80; $(C_3H_3CuN_2O_2)^+$ M^+ 162.30; $(C_3H_4N_2O_2)^+$ M^+ 100; $(Cu)^+$ M^+ 63; $(C_6H_6)^+$ M^+ 78.11; $(C_3H_6)^+$ M^+ 42.01 (Fig S22).

2.5.8. L-4-Ni complex

M.P > 300 °C; Color; Brown; Yield: 57%: Solubility: DMSO. FTIR (cm^{-1}); NH: 3377; CH Sp_2: 3087; C=O: 1727; N=N: 1592; Cl: 834 Ni–O: 591 Ni–N: 424 (Fig S19).

2.6. Biological activity

Newly prepared azo derivatives and their metal complexes were screened out for antioxidant, antifungal and antibacterial activities. The stock solutions of understudy azo derivatives and their copper complexes (1 mg/mL) were prepared by the addition of 10 mg of azo compound in 10 mL DMSO. Then further dilutions were made according to the requirement of assays as reported in literature [41, 43, 44].

2.6.1. Antimicrobial assay

Three bacterial strains (*Escherichia coli, Salmonella typhi* and *Bacillus subtilis*) and three fungal strains *(Candida albicans*, *Candida glabrata*, and *Aspergillus niger*) were selected for antibacterial and antifungal assays respectively. The assay was performed by using disc diffusion method. The microbial strains were characterized by growing on nutrient agar medium. The solvent containing bacterial culture was autoclaved for 30 min at 115 °C and 15 lbs. pressure before inoculation. The agar medium was mixed with inoculums homogeneously and shifted on sterilized petri plates and incubated over night at 37 °C. Bacterial growth was shown under electron microscope. Ciprofloxacin and Fluconazole used as standard medicines for antibacterial and antifungal assays. Different concentrations of tested compounds and standard (3–1.5 mg/mL) in dried DMSO was added drop wise into filter paper having 6 mm diameter disc positioned in the center of agar plates and marked properly and these agar plates were incubated for 24 h at 37 °C. Transparent zone around each disk represented the inhibition activity of test compounds [45, 46, 47]. After incubation zones were formed and measured with the help of scale. The assay was performed in triplicate and the average was taken as the final reading.

2.6.2. DPPH radical scavenging activity

Antioxidant activities of understudy azo derivatives, their metal complexes was determined by adopting reported procedure by H. Ammara *et.al* [42, 48]. For this purpose, 0.3 mmol solution of DPPH was prepared by mixing 11.5 mg of DPPH in ethanol and kept in dark. The solution of 1000 ppm of azo derivatives, metal complexes and standard (Ascorbic acid) were prepared by mixing 0.01g in 10 mL of DMSO, then different concentrations (50, 100, 150, 200, 250 μg/mL) were prepared by dilution method. From the stock solution 10 μL of each understudy azo derivative, solvent blank and standard were taken in microtiter plate. DPPH (0.3 mmol) 100 μL solution was added into sample and standard and kept at 37 °C for 45 min to generate free radical. At 517 nm absorbance was measured using ELISA micro plate reader and the measurements were done in triplicate manner. Scavenging capacity of understudy azo derivatives was measured by comparing it with standard (Ascorbic acid) and solvent blank. Results were given in % inhibition after calculated by equation below:

$$\text{Inhibition}\% = \text{Absorbance}_{\text{blank}} - \text{Absorbance}_{\text{sample}} \times 100 / \text{Absorbance}_{\text{blank}}$$

3. Result and discussion

3.1. Chemistry

Four new azo ligands were synthesized by using 2-amino-3-chlorobenzophenone and 2-amino-3,5-dichlorobenzophenone as aniline and barbituric acid and thio-barbituric acid as coupling reagent using reported method [41, 49]. Colored azo ligands were synthesized successfully to be soluble in ethanol, methanol and DMSO solvents. By using the azo ligands, CuII) and Ni(II) metal complexes were synthesized. All metal complexes found to be soluble in DMSO. All are colored solid, stable and non-hygroscopic in nature. Melting points of ligands were higher than 150 °C and less than 300 °C but all metal complexes have melting points greater than 300 °C. Analytical data suggests that in metal complexes M to L ratio (metal to ligand ratio) is 1: 2 stoichiometrically having $(M(L)_2)$ type metal complexes for deprotonated ligands [50]. Preparation of azo ligands and their metal complexes was verified persuasively form various analytical techniques such FTIR, ^{1}H NMR, ^{13}C NMR and mass spectrometry.

3.2. FTIR spectral study

FTIR spectra of azo ligands (HL1-HL4) illustrated that the azo ligands are also stable in the form of azo keto-enol both in solid as

well as in solution state due to appearance of hydroxyl stretching frequency in the range of 3000–3350 cm^{-1}. Furthermore, disappearance of $–NH_2$ peaks and appearance of N=N new peaks at 3450-3550 cm^{-1} and 1390-1520 cm^{-1} respectively also gives strong indication for the synthesis of compounds along with other peaks at their proper positions [51] as shown in Figure 1a and Fig S1-S4. On complexation with metals the band appeared for azo groups (N=N bond) at 1390-1520 cm^{-1} were shifted almost at 30-40 cm^{-1} towards lower wavelength, proved the involvement of azo group in coordination with metal. In free ligands the –OH absorption band that appeared at 3200–3300 cm^{-1} of phenolic group, were vanished in entirely metal complexes indicated the development of bond amongst oxygen of phenolic group and metal ion through deprotonation [52]. The absorption band for phenolic oxygen and carbon (C–O) appeared at 1100–1200 cm^{-1} also shifted towards lower wave length about 40–50 cm^{-1} in all metal chelates. This is also confirmed the formation of metal complexes. Two most important peaks (M-O, M-N) appeared in all the metal chelates in the range of 400–600 cm^{-1} which were not present in any of the ligand [53]. The absorption bands for C=O and NH- appeared at the same region in metal chelates and in free ligands showed their non-involvement in the coordination process as given in Figure 2 and Fig S5-12.

3.3. ^{1}H NMR spectral study

^{1}H NMR spectroscopy is also a superb technique for the confirmation of synthesized azo ligands by comparing the spectra of reactants and products. The spectra were measured in DMSO. The azo ligands showed singlet peak at 11.5–13.5 ppm (s IH, Ar-OH) for hydroxyl group also established the keto enol form of synthesized azo compounds. Vanishing of $–NH_2$ group signals at 4–5 ppm correspondingly, established the synthesized azo compounds as given in Figure 1b & Fig S4-S6. Doublet peak appeared at 8.5–9.5 ppm (d, 2H, NH) for NH. The signals due to benzene protons (m 20H, Ar–H) appeared as multiplets in the range of 6.21–8.00 ppm [54]. Therefore, from ^{I}H NMR it was evident that the proposed structure was in excellent agreement with spectral data and gives strong indication for the formation of ligands.

3.4. ^{13}C NMR spectral study

^{13}C NMR analysis were performed for the confirmation and existence of synthesized azo compounds (HL1-HL4) and existence of keto-enol form also verified by ^{13}C NMR analysis, due to the presence of sharp signals of carbon having –OH group appeared in the range of 180–192 ppm. Carbon atoms in the aryl ring appeared in the range of 125–150 ppm. Carbon attached with nitrogen appeared in the range of 100–105 ppm [55] as shown in Fig 1c & Fig S7-S9.

3.5. Mass spectral study

For the determination of exact molecular mass of synthesized compounds mass spectrometry technique is very essential tool from which we can also identify the mode of fragmentation. The spectra of azo ligands (HL1-HL4) and their Cu(II) complexes displayed that molecular ion peaks are according to their purposed molecular formula. The spectra of representative azo ligand (HL-1) exhibited molecular ion peak ~~due to~~ M^+ at m/z 372 which is the molecular weight of azo ligands as shown in Figure 1d and Fig S10-S12 and mode of fragmentation given in Scheme 3 and Scheme S1-3. The mass spectra of other azo ligands (HL2-HL4) presented molecular ion peaks ~~due to~~ M^+ at m/z 388, 407 and 423 which are according to their molecular masses as shown in Fig S23-26, and their mode of fragmentation also shown in Scheme S1-3 and In the same way the mass spectra of metal complexes also in good agreement with their molecular weight. The spectra of L1-Cu to L4-Cu showed molecular ion peaks ~~due to~~ M^+ at m/z 803, 835, 871 and 904 which are equivalent to their molecular mass of respective compounds. The mass spectra of complexes, the Cu (II) ion peak also appeared which confirmed the presence of Cu-metal [56] as shown in Figure 3 and Fig S20-23. The mass fragmentation pattern of above metal complexes is presented in Scheme 4 and scheme S4-6 provided in supplementary data.

4. Pharmacological studies

4.1. Antimicrobial studies

In-vitro antimicrobial studies of new series of azo ligands and their Cu(II) and Ni(II) complexes screened out against three bacterial strains *E. coli*, *S. typhi*, and *B. subtilis* and three fungal strains *C. albicans*, *A. niger*, and *C. glabrata*. Results are presented in Tables 1 and 2 Table S1-2 and indicated that all the understudy azo compounds showed variable inhibitory effect against all the pathogens. It was observed that although all the four ligands showed good antimicrobial activity as compared to standard drugs but metal chelates exhibited excellent activity as compared to free ligands and standards. Regarding the structural activity relationship of azo ligands (HL-1 to HL-4) exhibited very good activity as compared to standard drugs against all the pathogens, because they have many electron withdrawing groups such as N=N, C=O, C=S, 2-Cl and 2, 5-dichloro. In this view order of activity of azo ligands is HL-4 > HL-2 > HL-3 > HL-1. In case of metal chelates, coordination of metal ions with free ligand enhances the inhibitory effect on the growth of pathogens because lipophilic character of metal chelates increases the polarity of cell wall that favors the penetration through the lipids layered of pathogen cell wall. Formation of hydrogen bond of nitrogen atom of N=N of target compounds with the active cite of enzymes of pathogen cell causes the disturbance in the normal cell process. Respiration procedure of cell also destructs, thus inhibit the protein synthesis which leads to stop the growth of pathogens [57]. Order of activity of metal chelates for *S. typhi and E. coli*, Cu(II) complexes is more active than Ni(II) complexes and for *B. subtilis,* Ni(II) complex is more active than Cu(II) complexes and standard. The

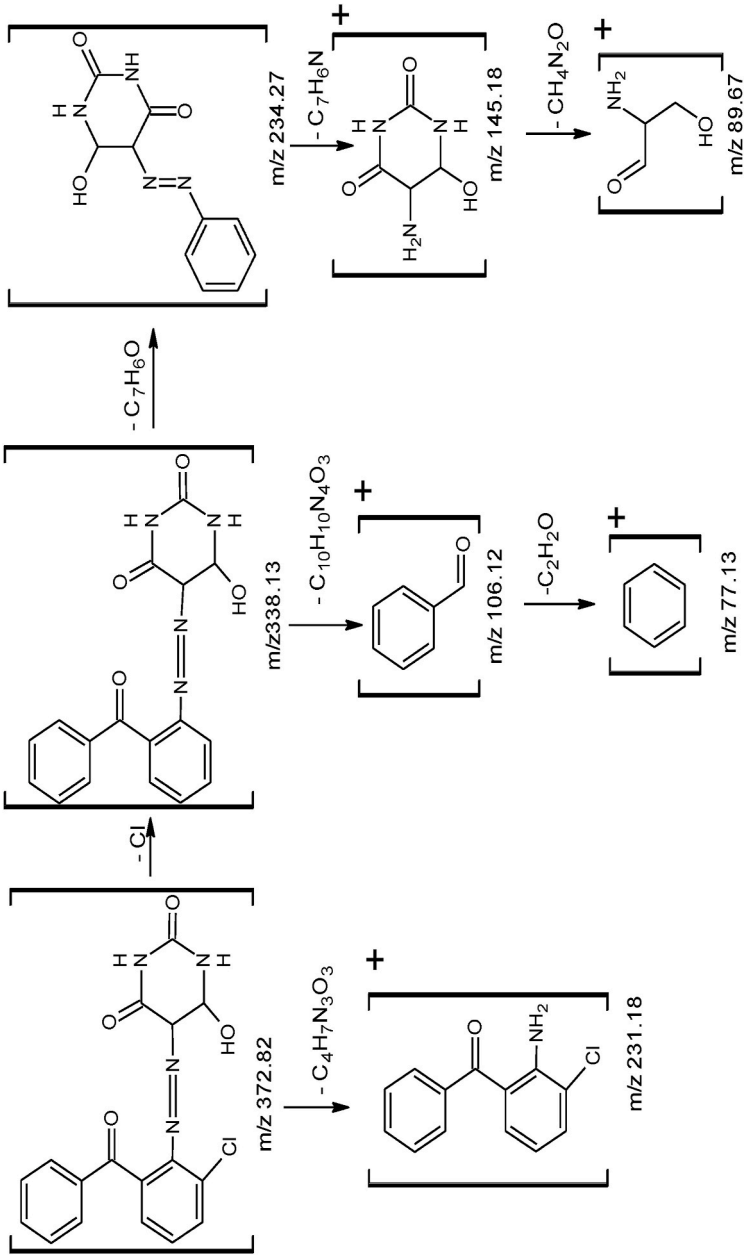

Scheme 3. Mass fragmentation pattern of ligand HL-1.

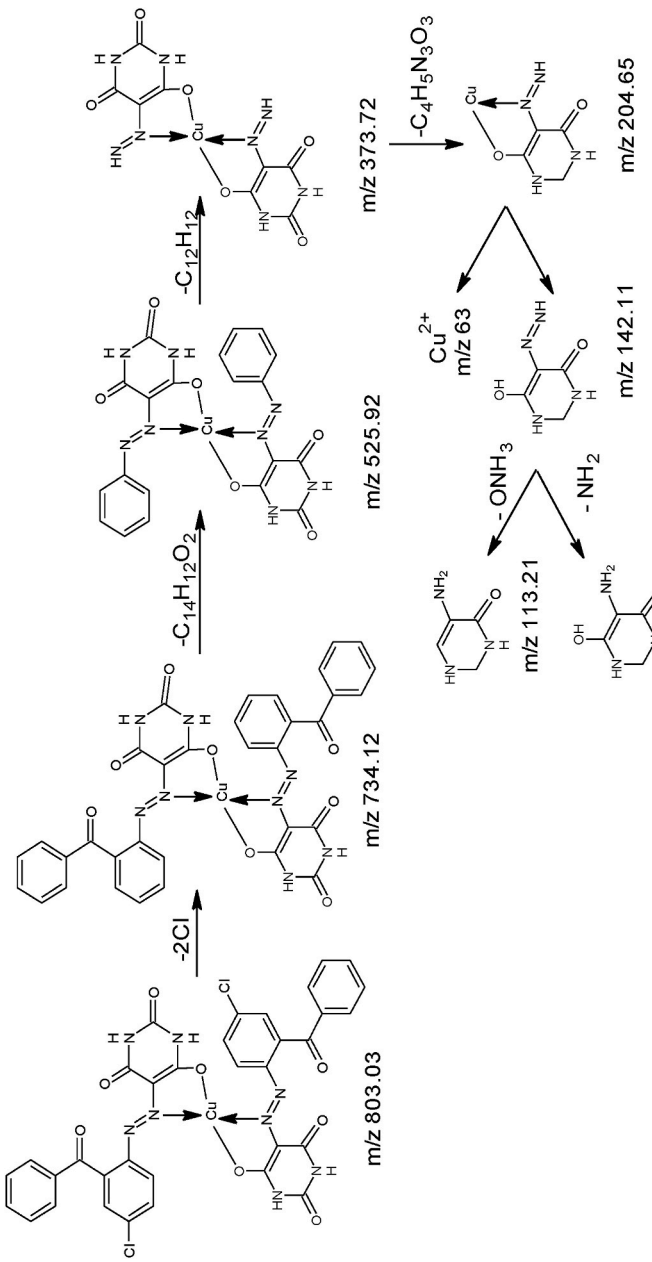

Scheme 4. Mass fragmentation pattern of L1-Cu.

Table: 1
Results of antibacterial activity of HL-1 ligand and its metal complexes.

Sr. No.	Sample code	Zone of inhibition in mm		
		E. coli	*S. typhi*	*B. subtilis*
1	HL-1	17	16	17
2	HL-1-Cu	28	27	24
3	HL-1-Ni	26	25	29
4	Ciprofloxacin	15	14	16

All compounds soluble in DMSO.
In this table mm = millimeter.

Table: 2
Results of antifungal activity of HL-1 ligand and its metal complexes.

Sr. No.	Sample code	Zone of inhibition in mm		
		C. glabrate	*C. albicans*	*A. niger*
1	HL-1	23	24	21
2	HL-1-Cu	27	25	23
3	HL-1-Ni	28	28	27
4	Fluconazole	22	20	19

All compounds soluble in DMSO.
In this table mm = millimeter.

anti-fungal study of Ni(II) complexes exhibits higher activity against all the three fungal strains *e.g. C. glabrate*, *C. albicans* and *A. niger* as shown in Tables 1 & 2.

4.2. DPPH radical scavenging activity

Antioxidant is the compound that inhibits metabolic disorder induced by free radical species. Synthetics antioxidants are exhibited more scavenging activities as compared to natural antioxidants. But their use is limited to their toxic effects. So, the chemists are interested to discover such synthetic antioxidants which are less toxic and more effective in nature than natural antioxidants. In this regard new class of azo derivatives and their metal complexes were screened for their scavenging capacity by using DPPH assay. Results of scavenging activity of under study compounds are presented in Table 3 and Table S-3. It was cleared from results that the activity is dose dependent [58, 59]. Among the under-study compounds activity order of ligands is HL-1 > HL-2 > HL-3 > HL-4 > A.A. In case of metal complexes Cu-complexes showed excellent activity and Ni-complexes showed moderate activity as compared with standard drug ascorbic acid.

5. Conclusion

In this study a new series of azo ligands with barbituric and thio-barbituric acid were synthesized successfully having excellent yield, in reproducible conditions at low temperature (05 °C) using coupling diazotization. Further these ligands were reacted with metal salts to produce metal complexes using reflux method. For the confirmation and structure elucidation of ligands and their transition metal complexes different advance spectroscopic techniques (FTIR, ^{1}H NMR, ^{13}C NMR and Mass Spectrometry) were applied. In FTIR analysis absence of NH_2 peak at 3450-3550 cm^{-1} and appearance of N=N peak at 1390-1520 cm^{-1} confirmed the synthesis of ligands. On complexation with metals the bands appeared at 1390-1520 & 1100-1200 cm^{-1} for azo group in case of ligands was shifted towards lower wavelength, proved the involvement of azo group in coordination with metal. Two most important peaks (M-O, M-N) appeared in all the metal chelates in the range of 400–600 cm^{-1} which were not present in any of the ligand confirmed the formation of complexes. In ^{1}H NMR the azo ligands showed singlet peak at 11.5–13.5 ppm (s IH, Ar-OH) for hydroxyl group and disappearance of $–NH_2$ signals at 4–5 ppm also confirmed the synthesis of azo ligands. In ^{13}C NMR analysis, due to the presence of sharp signals of carbon having OH group appeared in the range of 180–192 ppm confirms the formation of ligands. Molecular ion peaks

Table 3
Results of antioxidant activities of HL-1 ligand and their metal complexes.

Sr. No.	Sample code	% Inhibition				
		50 μM	100 μM	150 μM	200 μM	250 μM
1	HL-1	49	63	69	74	76
2	HL-1-Cu	55	67	73	79	88
3	HL-1-Ni	52	63	70	75	82
6	Ascorbic Acid	46	56	62	68	72

All compounds are soluble in DMSO.

in mass spectrometry at 273, 388, 407 and 423 m/z for ligands as well as for complexes at 803, 835, 871 and 904 m/z also give strong indication that proposed ligands and their metal complexes are produced successfully. Biological screening of these synthesized ligands and metal complexes were carried out against antibacterial (*E. coli*, *S. typhi*, and *B. subtilis)* and antifungal (*C. albicans*, *A. niger*, and *C. glabrata)* strains as well as antioxidant activities. From results it was observed that HL-4 exhibited maximum inhibition against all bacterial strains as compared to other ligands as well as standard drug. Ligand HL-4 also showed maximum inhibition against all fungal strains except *C. albicans* and against this strain ligand HL-1 showed highest inhibition capacity. In case of antioxidant all ligands exhibited almost same and higher activity than standard drug. In case of metal complexes all compounds showed excellent inhibition activities against fungal and bacterial strains as well as antioxidant activities greater than ligands and standard medicine. Among all metal complexes Cu-complexes exhibited remarkable activities against bacterial and fungal strains as well as antioxidant activity. From this study it was revealed that these synthesized azo ligands as well as their metal complexes can be applied successfully to get rid of complications and diseases produced from these pathogens.

Declarations

Author contribution statement

Tariq Aziz, Hafiza Ammara Nasim: Performed the Experiments; Wrote the Paper.
Khalil Ahmad, Muhammad Ashfaq: Conceived and Designed the Experiments; Analyzed and Interpreted the Data.
Habib Ur Rehman Shah, Ahmad M. Galal: Contributed Reagents, Materials, Analysis Tools or Data.
Sajidah Parveen: Performed the Experiments.
Muhammad Mahboob Ahmad, Hammad Majeed, Abdul Rauf: Analyzed and Interpreted the Data.

Funding statement

This research did not receive any specific grant from funding agencies in the public, commercial, or not-for-profit sectors.

Data availability statement

No data was used for the research described in the article.

Declaration of interests statement

The authors declare no competing interests.

Additional information

Supplementary content related to this article has been published online at https://doi.org/10.1016/j.heliyon.2022.e12492.

Acknowledgements

Authors are highly grateful to Institute of Chemistry, Baghdad ul Jadeed Campus, The Islamia University of Bahawalpur, Pakistan for providing all facilities to complete this project.

References

[1] D. Ganguly, et al., Radioprotection of thymine and calf thymus DNA by an azo compound: mechanism of action followed by DPPH radical quenching & ROS depletion in WI 38 lung fibroblast cells, Heliyon 6 (5) (2020), e04036.
[2] X. Li, Y. Wang, Q. Guo, Porous NH2-MIL-101(Fe) metal organic framework for effective photocatalytic degradation of azo dye in wastewater treatment, Heliyon 8 (7) (2022), e09942.
[3] S. Benkhaya, S. M'Rabet, A. El Harfi, Classifications, properties, recent synthesis and applications of azo dyes, Heliyon 6 (1) (2020), e03271.
[4] H. Ren, et al., The detection of multiple analytes by using visual colorimetric and fluorometric multimodal chemosensor based on the azo dye, Heliyon 8 (8) (2022), e10216.
[5] O. Nagaraja, et al., Synthesis, characterization and biological investigations of potentially bioactive heterocyclic compounds containing 4-hydroxy coumarin, Heliyon 6 (6) (2020), e04245.
[6] F. Al-Haj Hussien, An eco-friendly methodology for the synthesis of azocoumarin dye using cation exchange resins, Heliyon 7 (11) (2021), e08439.
[7] B. Devika, et al., Synthesis, characterisation and molecular structure study of metal complexes of antipyrine based ligand 1185, 2019, pp. 69–77.
[8] S. Kansiz, et al., Crystal structure and Hirshfeld surface analysis of 2-methyl-3-nitro-N-[(E)-(5-nitrothiophen-2-yl) methylidene] aniline 77, 2021, pp. 138–141 (2).
[9] K. Ahmad, et al., Comparative study between two zeolitic imidazolate frameworks as adsorbents for removal of organoarsenic, as (III) and as (V) species from water 9, 2022, pp. 78–97.
[10] N. Mallikarjuna, et al., Synthesis, characterization, thermal and biological evaluation of Cu (II), Co (II) and Ni (II) complexes of azo dye ligand containing sulfamethaxazole moiety 1165, 2018, pp. 28–36.
[11] A. Haque, et al., Synthesis, characterization, and pharmacological studies of ferrocene-1H-1, 2, 3-triazole hybrids 1146, 2017, pp. 536–545.

[12] D. Douche, et al., 5-((1H-imidazole-1-yl) Methyl) Quinolin-8-Ol as Potential Antiviral SARS-CoV-2 Candidate: Synthesis, crystal Structure, Hirshfeld Surface Analysis, DFT and Molecular Docking Studies 1232, 2021, 130005.
[13] A. Ayub, et al., Arsenic in Drinking Water: Overview of Removal Strategies and Role of Chitosan Biosorbent for its Remediation, 2022, pp. 1–33.
[14] Z. Ahmad, et al., Pod Shattering in Canola Reduced by Mitigating Drought Stress through Silicon Application and Molecular Approaches-A Review, 2022, pp. 1–28.
[15] N. Mallikarjuna, J.J. Keshavayya, Synthesis, spectroscopic characterization and pharmacological studies on novel sulfamethaxazole based azo dyes, J. King Saud Univ. Sci. 32 (1) (2020) 251–259.
[16] Y. Oueslati, et al., Synthesis, crystal structure, DFT calculations, Hirshfeld surface, vibrational and optical properties of a novel hybrid non-centrosymmetric material (C10H15N2) 2H2P2O7 1196, 2019, pp. 499–507.
[17] S. Rana, et al., Nutritional Assessment Among Undergraduate Students of the Islamia University of Bahawalpur 5, 2020, p. 2.
[18] S. Rana, K. Ahmad, H.M. Asif, K. Ahmad, A. Wadood, Nutritional Assessment among Undergraduate Students of the Islamia, University of Bahawalpur, J. Food Nutr. Disor. 9 (5) (2020) 2.
[19] G. Nagesh, K.M. Raj, B.J. Mruthyunjayaswamy, Synthesis, characterization, thermal study and biological evaluation of Cu (II), Co (II), Ni (II) and Zn (II) complexes of Schiff base ligand containing thiazole moiety, J. Mol. Struct. 1079 (2015) 423–432.
[20] U. Nazim, et al., Synthesis, characterization and cytotoxic effect of some new thiazolyl hydrazone derivatives of 1-indanone 43, 2021 (2).
[21] H.G. Sogukomerogullari, et al., Synthesis of complexes Fe, Co and Cu supported by "SNS" pincer ligands and their ability to catalytically form cyclic carbonates 471, 2018, pp. 290–296.
[22] N. Dege, H. Içbudak, E. Adıyaman, Bis (acesulfamato-κ2O4, N) bis (3-methylpyridine) copper (II), Acta Crystallograph. Sec. C: Crystal Struct. Commun. 62 (9) (2006) m401–m403.
[23] G. Swati, et al., Synthesis, characterization and antimicrobial screening of some azo compounds 2, 2011, pp. 332–338 (2).
[24] D. Avcı, et al., A Novel Series of Mixed-Ligand M (II) Complexes Containing 2, 2′-bipyridyl as Potent α-glucosidase Inhibitor: Synthesis, crystal Structure, DFT Calculations, and Molecular Docking 24, 2019, pp. 747–764 (5).
[25] E. Aydemir, et al., Crystal structure and Hirshfeld surface analysis of 7-ethoxy-5-methyl-2-(pyridin-3-yl)-11, 12-dihydro-5, 11-methano [1, 2, 4] triazolo [1, 5-c] [1, 3, 5] benzoxadiazocine 74 (3) (2018) 367–370.
[26] K. Ahmad, et al., Assessment of Nutritional Status of Undergraduate Students of the, Islamia University Bahawalpur, 2021, pp. 32–43.
[27] M. Chaudhary, et al., Synthesis and antibacterial activity of 1-(2-Diazo-6-ethoxybenzothiazolyl) substituted benzene derivatives 1, 2010, pp. 175–179.
[28] K. Ahmad, et al., Synthesis of New Series of Phenyldiazene Based Metal Complexes for Designing Most Active Antibacterial and Antifungal Agents 43, 2021 (5).
[29] N.B. Arslan, et al., Direct and solvent-assisted thione–thiol tautomerism in 5-(thiophen-2-yl)-1, 3, 4-oxadiazole-2 (3H)-thione: experimental and molecular modeling study 439, 2014, pp. 1–11.
[30] M. Ashfaq, et al., Synthesis, crystal structure, Hirshfeld surface analysis, and computational study of a novel organic salt obtained from benzylamine and an acidic component 6, 2021, pp. 22357–22366 (34).
[31] J. Sahoo, S.K.J. Paidesetty, Antimicrobial activity of novel synthesized coumarin based transitional metal complexes, J. Taibah Univ. Med. Sci. 12 (2) (2017) 115–124.
[32] K. Ahmad, et al., Lead in Drinking Water: Adsorption Method and Role of Zeolitic Imidazolate Frameworks for its Remediation: A Review, 2022, 133010.
[33] T. Najam, et al., Metal-Organic Frameworks Derived Electrocatalysts for Oxygen and Carbon Dioxide Reduction Reaction, 2022, p. e202100329.
[34] G. Demirtaş, et al., Experimental and DFT Studies on Poly [di-M3-Acesulfamato-O, O: O′; O′: O, O-Di-μ-Acesulfamato-O, O; N-Di-μ-Aqua-Dicalcium (II)] Complex 22, 2012, pp. 671–679 (4).
[35] A. Ahmed, et al., Biocidal polymers (I): preparation and biological activity of some novel biocidal polymers based on uramil and its azo-dyes 68, 2008, pp. 248–260 (1).
[36] A.M. Fallatah, et al., Rational synthesis and characterization of highly water stable MOF@ GO composite for efficient removal of mercury (Hg2+) from water 8, 2022, e10936 (10).
[37] F. El Kalai, et al., Synthesis, crystal structure, spectroscopic studies, NBO, AIM and SQMFF calculations of new pyridazinone derivative 1223, 2021, 129213.
[38] S. Crespi, N.A. Simeth, B.J.N.R.C. König, Heteroaryl Azo Dyes as Molecular Photoswitches 3, 2019, pp. 133–146 (3).
[39] K. Naseem, et al., Investigation of catalytic potential of sodium dodecyl sulfate stabilized silver nanoparticles for the degradation of methyl orange dye 1262, 2022, 132996.
[40] P. Sen, et al., Peripherally tetra-benzimidazole units-substituted zinc (II) phthalocyanines: synthesis, characterization and investigation of photophysical and photochemical properties 194, 2018, pp. 123–130.
[41] K. Ahmad, et al., Synthesis and spectroscopic characterization of medicinal azoderivatives and metal complexes of Indandion, J. Mol. Struct. 1198 (2019), 126885.
[42] H.A. Naseem, et al., Rational synthesis and characterization of medicinal phenyl diazenyl-3-hydroxy-1h-inden-1-one azo derivatives and their metal complexes, J. Mol. Struct. 1227 (2021), 129574.
[43] M.A. Saeed, et al., DNA interaction and biological activities of heteroleptic palladium (II) complexes 43, 2021 (2).
[44] Z. Afzal, N. Rashid, H.J. Nadeem, Stereoselective synthesis, spectral characterization, docking and biological screening of coumarin derivatives, J. Chem. Soc. Pakistan 43 (3) (2021).
[45] H.U.R. Shah, et al., Free radical scavenging, antibacterial potentials and spectroscopic characterizations of benzoyl thiourea derivatives and their metal complexes 1272, 2022, 134162.
[46] S. Gopalakrishnan, et al., Antibacterial activity of azo compounds synthesized from the natural renewable source, cardanol 3 (4) (2011) 490–497.
[47] S.F. Thaokar, et al., Synthesis and antibacterial activity of novel pyrazolo [3, 4-b] quinoline based heterocyclic azo compounds and their dyeing performance 15, 2007, pp. 48–54 (1).
[48] A.D. Khalaji, et al., Mononuclear Copper (I) Schiff Base Complex Cu ((Cl-NO2-ba) 2en) I (CH3CN): synthesis and Crystal Structure 43, 2021 (1).
[49] R. Bibi, et al., Palladium catalyzed synthesis of phenylquinoxaline-alkyne derivatives via sonogashira cross coupling reaction 43, 2021 (1).
[50] A. El-Sonbati, M. Diab, S.M.J. Morgan, Thermal properties, antimicrobial activity and DNA binding of Ni (II) complexes of azo dye compounds, J. Mol. Liquids 225 (2017) 195–206.
[51] R. Zhao, et al., One step synthesis of azo compounds from nitroaromatics and anilines 52, 2011, pp. 3805–3809 (29).
[52] A. Grirrane, A. Corma, H.J.S. García, Gold-catalyzed synthesis of aromatic azo compounds from anilines and nitroaromatics 322, 2008, pp. 1661–1664 (5908).
[53] N.M. Aljamali, Review in azo compounds and its biological activity, Biochem. Anal. Biochem. 4 (2) (2015) 1–4.
[54] H.U.R. Shah, et al., Synthetic routes of azo derivatives: a brief overview 1244, 2021, 131181.
[55] E. Merino, Synthesis of azobenzenes: the coloured pieces of molecular materials, Chem. Soc. Rev. 40 (7) (2011) 3835–3853.
[56] Y. Zhu, Y.J.O.l. Shi, Facile Cu (I)-catalyzed oxidative coupling of anilines to azo compounds and hydrazines with diaziridinone under mild conditions, Organic Lett. 15 (8) (2013) 1942–1945.
[57] R. Gup, et al., Synthesis and spectroscopic properties of new azo-dyes and azo-metal complexes derived from barbituric acid and aminoquinoline, Dyes Pigm. 73 (1) (2007) 40–46.
[58] W.H. Mahmoud, et al., Synthesis, spectral characterization, thermal, anticancer and antimicrobial studies of bidentate azo dye metal complexes 124, 2016, pp. 1071–1089 (2).
[59] K. Ahmad, et al., Engineering of Zirconium based metal-organic frameworks (Zr-MOFs) as efficient adsorbents 262, 2020, 114766.